Design of an in-wheel propulsion concept for an electric racecar

Carl P-Conquilla
20768592
School of Mechanical and Chemical Engineering
University of Western Australia

Supervisor: Associate Professor Adam Wittek
School of Mechanical and Chemical Engineering
University of Western Australia

Engineering Project Report
MECH3402
School of Mechanical and Chemical Engineering
University of Western Australia

Submitted: Semester Two, 2014

Contents

THE UNIVERSITY OF WESTERN AUSTRALIA

Dear Associate Professor Wittek,

I hereby declare that the design of the planetary differential input transmission mechanism, the conception of the laminar helical approximation arrangement and the research compiled within this report as submitted are solely my own work.

-Carl P-Conquilla, 31 October 2014

1 Abstract

Due to the failure of an in-wheel propulsion system in the 2013 UWA Formula REV racecar a new design was called for with the primary focus of a higher electrical efficiency, whilst being adjustable for packaging purposes and to be manufactured at extremely low cost.

After evaluating possible solutions such as a centrifugal clutch, multi-ratio gearbox, continuously variable transmission, soft start sequence or torque converter, it was decided that a differential mechanism would be used to allow two motors to rotate at near their highest efficiency throughout their range of operation.

In order to minimise costs throughout the proof of this prototype, the manufacture of traditional high tolerance components such as gears and bearings is also revisited. Given the short operating life and high demands of the racecar, these items when manufactured following this revised method are considered nearly consumable and replaced regularly.

The purpose of this project is to:

- Discuss the concept of an in-wheel four wheel drive for Formula SAE
- Analyse and assemble a prototype propulsion design
- Test the design for operational suitability and report findings
- Propose a system that incorporates the propulsion design into the wheel assembly (recommendations for future work)

The novel and distinct feature of this in-wheel propulsion system is that it features not one, but two motors within each wheel. This holds a few advantages which will be discussed with the context of the transmission that couples them.

2 Electric Propulsion Today

Electric propulsion has advantages of power density and packaging flexibility over traditional internal combustion vehicles. This is clear with new technology such as the Tesla Model X, which features impressive power and storage space due to the advantages of electric vehicle architecture.

Other benefits of this technology include the capability to fit entire propulsion and transmission systems in-wheel (within the wheel assembly of the vehicle). This is becoming an increasingly common research subject for universities and military technology developers around the world.

This is because not only does electric vehicle technology demonstrate steps towards environmental sustainability, but it provides promise in areas demanding high performance. For example, compact and distributable propulsion units mounted in-wheel avoid complex and bulky mechanical transmission, allow for a more flexible vehicle mass distribution, and offer high speed digital control for tractive response applications, just to name a few.

2.1 Existing and relevant solutions

The Formula SAE competition takes place internationally, uniting over 500 university teams to develop highly performing racecars in the name of engineering. Each year since 2012, racecars in the in-wheel electric category have clearly outshone their internal combustion counterparts in elements of traction, acceleration, endurance and autocross circuit racing. (FSAE Results)

In-wheel propulsion systems present many attractive opportunities for automotive designers. In-wheel propulsion allows for flexibility with driven wheel configurations such as front-wheel, rear-wheel and all-wheel drive vehicles. The compact size also allows more packaging room within the rest of the vehicle that would traditionally be occupied by transmission systems, or allow for overall smaller and lighter vehicles without these systems. The response of in-wheel propulsion systems also favours highly advanced vehicle control concepts such as traction control, torque distribution, and active differential control. (Mraz, 2013)

In electric vehicles, the traditional differential mechanism can be omitted by having two motors each providing torque through an electronic differential controller. The disadvantage of this is that the cost of a motor per kilowatt is considerably more for smaller motors than for large ones. (Larminie and Lowry, 2003)

The major disadvantage to an in-wheel propulsion system is the increase in unsprung mass due to the addition of components to the wheel. Increases in unsprung mass are predicted to reduce handling characteristics of the car, as the increased mass is less responsive in conforming to changes in the road surface. The mass of in-wheel propulsion system regardless of its configuration is significantly impacted by the mass of the magnets in the electric motor in the system. As the use of alloys or composite components can be used to make transmission, suspension and structural components lighter; magnets for this purpose are very difficult to produce any lighter than they already are. (Mraz, 2013)

(Protean Paper) In general, there are two different possibilities of realizing an electric wheel-hub drive: low-speed direct drive or high-speed drive incorporating an additional gear-box. In this paper, these two alternatives are compared concerning weight, volume, and complexity for a typical mid-class passenger car. For this application, weight is one of the most important parameters, because the unsprung mass is increased with (at least in principle) negative effects on the driving performance of the car.

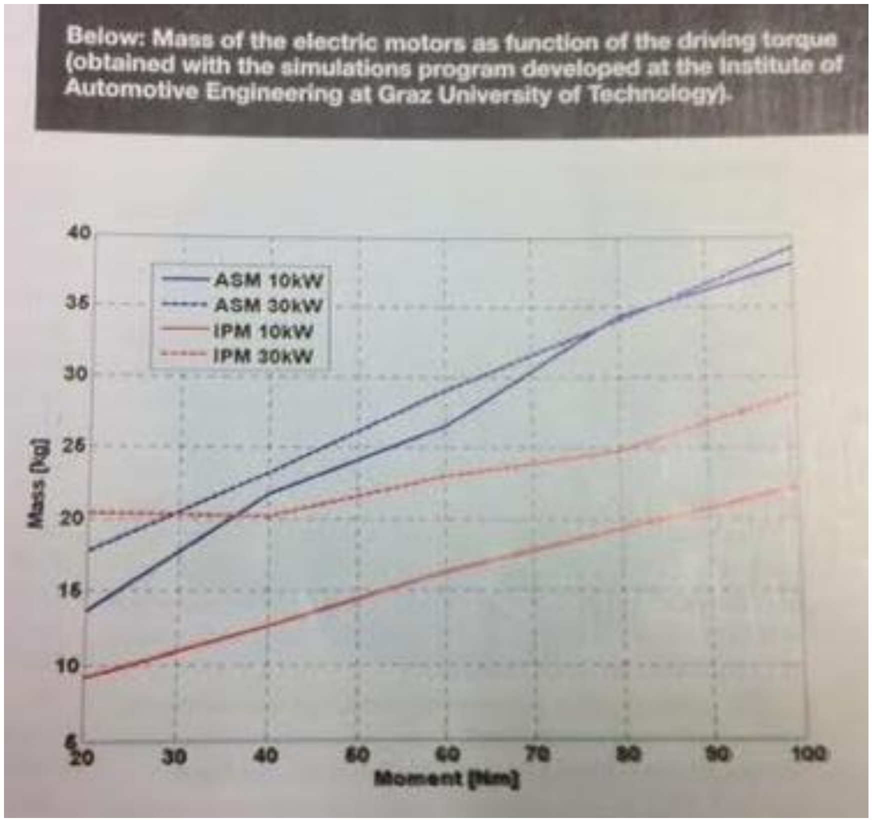

Figure 1 – The relationship between motor mass and torque via simulations (Automotive Engineering, Feb 2011 pg.31)

Lastly, for this project all in-wheel assemblies will be designed with the same package albeit symmetrically, for the left and right hand side assemblies. Whilst different packaging applied to front and rear wheel sets may be beneficial in lowering the assembly mass and overall vehicle mass, the additional design complexity and cost associated with this, and the increase in the number of unique components required brings forth concerns over budget, additional manufacturing requirements and the cost of spares.

2.2 Comparison of existing design with existing/relevant designs

From Figure 1 it can be seen that motors become more efficient as their mass (and consequently size) increases. (Larminie and Lowry, 2003) also states that efficiency generally increases for motors designed for high-speed operation than for low-speed operation.

Also from the two styles of electric motor designs, there are higher losses in a low-speed/high torque motor, than the converse configuration for a given power.

Larminie and Lowry state that small efficiency gains (in the order of 1%) can be made by liquid cooling the motor windings reducing their internal resistance.

Another factor in electric motor selection is that larger motors take more time to heat up, smaller motors heat up very quickly comparatively. This means that larger motors usually are capable of peak or near-peak output for much longer than smaller motors.

According to Larminie and Lowrie's claims, "[motors] can be safely driven well in excess of their rated power for short periods... this must not be overdone, otherwise local heating could cause damage.

"Higher powers are often only required are often only required for short time intervals, such as when accelerating." This suggests that majority of the capacity of electric motors for electric vehicles are largely over-specified, and this is a major contribution to the mass of the motor and consequently to the whole vehicle.

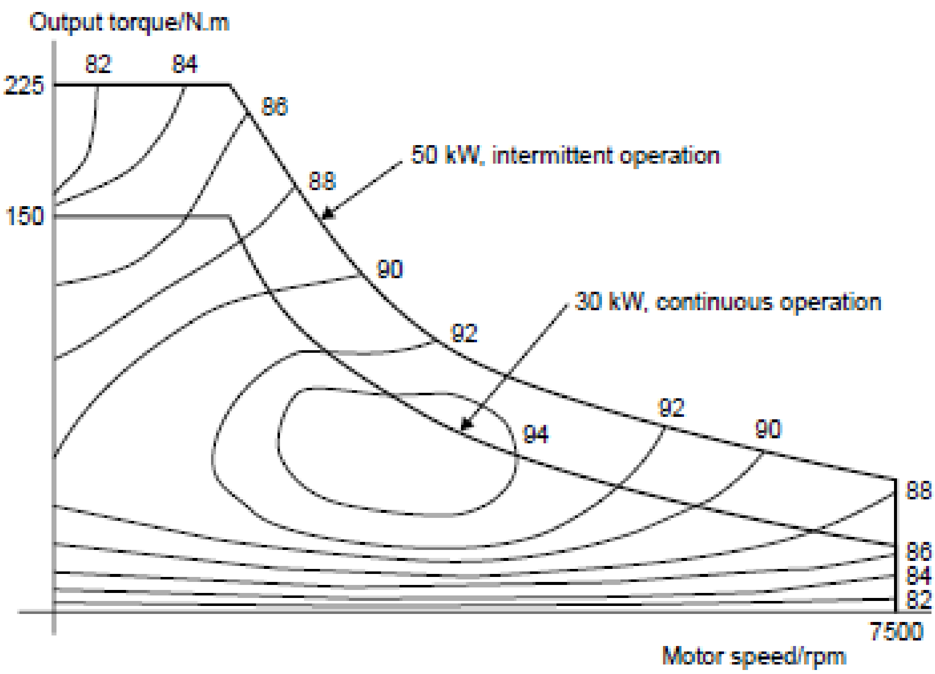

Figure 2 - The efficiency map for a 30kW BLDC motor. This is taken from the manufacturer's data, but note that in fact at zero speed the efficiency must be 0%. (Larminie and Lowry, 2003)

Efficient motors are appealing because they result in less waste heat to dispose of, resulting in an overall smaller and lighter motor. For example, a small and efficient motor could be comparable to a larger less efficient motor, where the large motor must be larger to dispose of more heat as well as make up for the output losses.

Power, kW	Minimum efficiency, %
1.1	83.8
2.2	86.4
4	88.3
7.5	90.1
15	91.8
30	93.2
55	96.2
90	95.0

Figure 3 – The minimum efficiency of four-pole three-phase induction motors to be classified as Class 1 efficiency under EU regulations. Efficiency measured according to IEC 36.2. (Larminie and Lowry, 2003)

It can be seen from Figures 3 and 4 that higher powered motors are innately more efficient. Motors designed for higher speeds have higher power density, and the size of the motor varies more for torque output than power. The example used by Larminie and Lowrie, is "that a higher speed, lower torque motor will be smaller. So if a low speed rotation is needed, a high speed motor with a gearbox will be lighter and smaller than a low speed motor."

"A good example is an electric vehicle, where it would be possible to use a motor directly coupled to the axle. However, this is not often done, and a higher speed motor is connected by (typically) a 10:1 gearbox." (Larminie and Lowry, 2003)

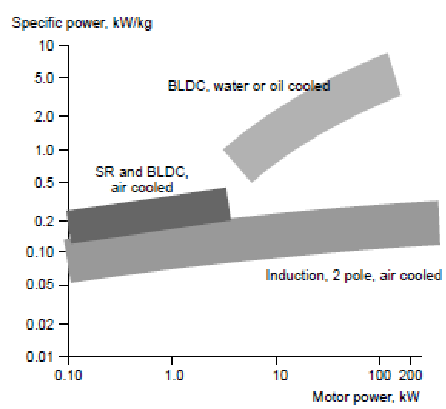

Figure 4 – Chart to show the specific power of different types of electric motor at different powers. The power here is the continuous power. Peak specific power is will be 50% higher. Note the logarithmic scales (this chart was made using data from several motor manufacturers).

Speed (rpm)	Mass (kg)
3000	270
1500	310
1000	415
750	570

Figure 5 – The mass of some 37kW induction motors, from the same manufacturer, for different speeds. The speed is for a 50Hz AC supply.

3 Acceptance of alternatives: Weighted evaluation matrix

In order to evaluate multiple alternatives quickly, certain criteria common to each solution were discussed. A score out of five was then given to each solution and then each criterion was weighted by its significance on the overall design objectives.

The score is calculated by multiplying each criteria weight by the score, and the sum of these scores results in a score total for each alternative. It is then clear which solution best meets the objectives of the design.

Criteria	Weight	Clutch	Multi-Ratio Transmission	Continuously Variable Transmission
Function Does it solve the problem?	5	The clutch allows the motors to spin up under no-load, but are fixed to one speed ratio (2)	A selectable gearbox has advantages of a very wide range of ratios (5)	A CVT allows a smooth delivery over a large ratio range (5)
Cost How much cost to build?	2	Readily available for similar applications, adaptation necessary (5)	Custom design or adaptation necessary (2)	Completely custom design necessary (2)
Reliability What kinds of failures?	4	Reputable (4)	Well understood concept (3)	Well understood concept (3)
Mass	1	Light (4)	Heavy (1)	Reasonably light (3)
Complexity Difficult to design, service, manage spares?	3	Low number of parts, mostly readily available (4)	High number of parts, mostly readily available (3)	Moderate number of parts, mostly complex machined (2)
Score Total		52	51	50

Criteria	Weight	Soft Start Control	Torque Converter	Differential Input
Function Does it solve the problem?	5	Soft start reduces the launch capability of the motor, but does reduce stall loads considerably (2)	Allows for smooth delivery of torque (5)	Provides a smooth delivery over a limited ratio range (4)
Cost How much cost to build?	2	Software control, little-to-no cost (5)	Completely custom design necessary (2)	Custom design or adaptation necessary (3)
Reliability What kinds of failures?	4	Only prolongs overheating, does not prevent it (2)	Well understood concept (3)	Well understood concept (3)
Mass	1	Massless (5)	Depends largely on execution (2)	Reasonably light (3)
Complexity Difficult to design, service, manage spares?	3	Software, easily implemented (5)	Moderate number of parts, mostly complex machined (2)	Moderate number of parts, mostly readily available (4)
Score Total		48	49	53

From this evaluation it is clear that a differential input mechanism would be the most suitable solution, closely followed by the clutch unit. The clutch was also an appealing option and may be considered more in depth in future iterations of the concept.

The inherent problem with gear components in this application is the cost of the fine machining process. Especially in the case of four in-wheel transmissions, the costs quadruple and become unfeasible even for small cost increases. The UWA Formula REV team addresses this problem by employing a new method for manufacturing gears.

The method was developed by the author as an attempt to find a compromise between the smooth meshing of helical gears and the manufacturability of spur gears, whilst reducing higher amplitude impulses from tooth bending and backlash, and minimising the effects of fracture propagation.

The method consists of a series of stacked laser cut gear laminations that are arranged such that the teeth of each gear are angularly offset from the gears either side of it. This arrangement represents a helical gear when the number of laminations is infinite, each lamination is infinitely thin, and the angular offset is constant throughout the stack. To the author's knowledge, the arrangement described has not been proposed before, and thus it will be referred to as the approximation of a helical gear through laminar gears.

The limitations of the process are that the laser cutting produces a very poor surface finish and inaccurate geometry when compared to high-performance machined gears. This limitation is accepted by the team and the author since the gears produced in this way are not expected to perform to as long service lives as those described in most gear machining literature; A Formula SAE event consists of four days worth of racing as opposed to (for example) 5000 hours of continuous operation that may be expected of perhaps a wind turbine.

Additionally, when the costs of manufacturing the gears themselves are considered; Approximately $200 per transmission leads the design to be considered a regular service replacement item, which could be reasonably be expected to be replaced once every six months of intermittent use.

4 Analyse and assemble a propulsion design:

In order to evaluate the suitability of the proposed manufacturing method, a prototype propulsion mechanism was produced. The design of this was intentionally rushed in order to demonstrate the feasibility within the time allocated for the project.

This means that the prototype first assembled had purposely omitted many important features of the transmission such as o-ring seals and mounting points.

There will be a design proposed at the end of this report that incorporates these considerations. The propulsion design as assembled consists of the motor rig, the transmission mechanism and the transmission case.

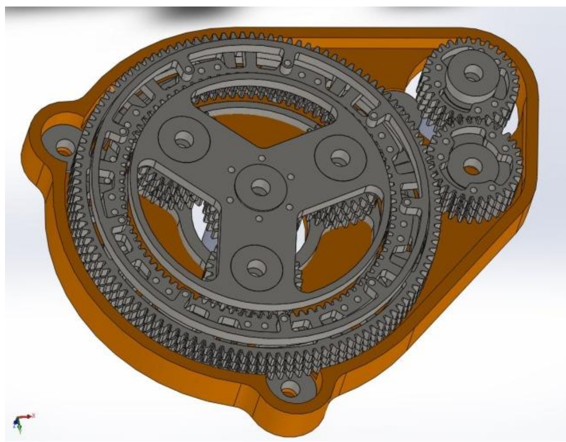

Figure 6 – The case and transmission design as developed in SolidWorks

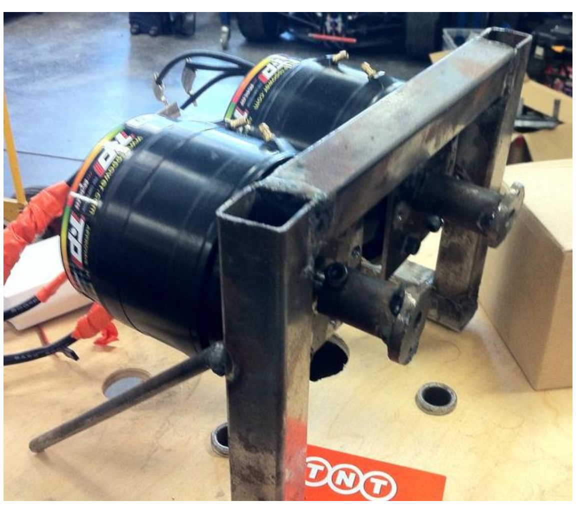

Figure 7 – The motors mounted to a testing rig. Shaft couplers were made to fit the 12mm shaft and three 3mm dowel pins.

Figure 8 – The transmission unit manufactured as per the design, in a case (half of the case has been removed). It weighs only 2.33kg.

4.1 Operation of the propulsion mechanism

The differential input mechanism is a rare mechanism, however it is not new. (Symes, H. 1958) reported a system that coupled two DC motors on a mechanically symmetrical epicyclic differential-gear unit, where the third element of the differential drives the wheels of a locomotive.

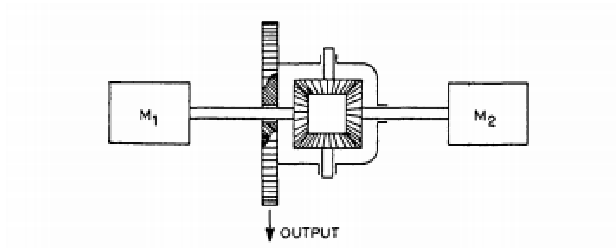

Figure 9 – Diagrammatic representation of a differential drive (Symes, H. 1958)

In Figure 9, M_1 and M_2 represent the two motors connected to the drive by a spider gear differential. According to Symes, any other type of differential could be used in place of the spider gear differential.

Symes describes step-by-step the operation of the mechanism:

"*Once started, the two motors run continuously for the duration of operation of the locomotive, in a direction such that the drive output is stationary when their speeds are equal. If no torque is developed for this condition the motors may be regarded as idling. Movement of the locomotive is then caused by a change in speed of either motor, the direction of travel depending on which pair runs the faster. The motors themselves are not stopped of reversed at any time.*"

The decision to implement this system in the racecar occurred in February 2014, and it was thought to be an original and novel concept conjured by the team. It was only in September 2014 that the author discovered the report by Symes in 1958 which had summarised and confirmed the speculations the team had made, and to the author's knowledge there are no other instances of a differential mechanism being used in this way.

Symes goes on to discuss the benefits of such a system:

"...The starting condition is noteworthy. The shunt fields may be set for full tractive effort at the wheels without moving the load. The armature speeds are then equal, the locomotive output is zero, and the current taken from the system is that

required for the losses only. The load is started from rest by a very small line current. The conditions of the well-known back-to-back test are thus reproduced at the commencement of acceleration. Once the load has been set in motion the motor-generator condition continues, but the rotor then runs faster than the generator.

"...An important feature of the stalled condition is that the machines are left running and their self-ventilation continues.

"...Except where specially mentioned, the effect of internal losses is disregarded, since the inclusion would not only complicate the analysis unnecessarily but would tend to obscure some of the more important basic features it is desired to emphasize.

"...It is impossible to overload the machines, since stalling occurs before this can happen, the load at the stalling point being suitably correlated with the rating.

Symes is essentially confirming the findings of the UWA Formula REV team in 2013 – The 2013 racecar experienced a major motor failure due to the high current conditions at stall. The method(s) proposed for solving this problem involved allowing the motors to escape from any stalled condition through idling or otherwise spinning the motor while the vehicle is stationary.

There are a number of other useful behaviours of this mechanism that Symes observed. A notable application for one of these in electric vehicles is that the mechanism can hold a torque at higher efficiencies than conventional methods in situations for example, a stationary locomotive on an incline,

4.1.1 Gear tooth calculations

The gear profiles used were generated by (RushGears.com, 2014), an online resource. The configuration parameters of the involute profile used were:

- Diametral Pitch: 20 teeth per inch of pitch diameter
- Pressure Angle: 14.5°
- Backlash: 0.003-0.005in
- Face Width: 3mm

4.1.2 Bending stress of teeth

To ensure the bending stress is at an allowable level, some realistic load cases are considered. Firstly, the maximum torque output of the two TP100 motors at the restriction of 21kW is 41.6Nm, and the expected torque at the output of the transmission will be 164Nm. This is in the case that the two motors are contributing in the same direction.

Additionally, the peak torque during launch may spike to much higher than the motor output momentarily and frequently. Therefore a safety factor of 2 is used.

Using the loose approximation that face_width = n * thickness_laminate, the load experienced by each gear is approximated to be 1/n the overall load transmitted between gears. Therefore the total load applied in the simulation is $(41.6 * 2)/6 = 13.87Nm$.

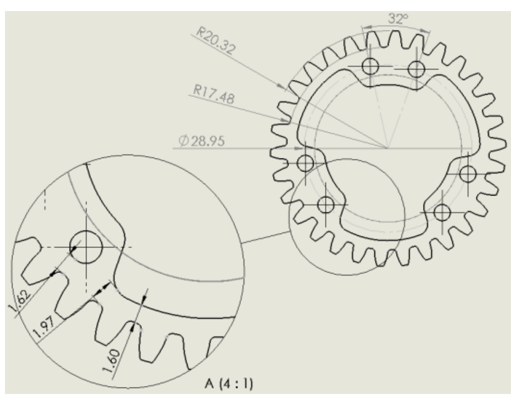

Figure 10 – Drawing indicating the backing material of the gear teeth in several places

As can be seen, the region with the least backing material is where a tooth root is present along the gear arc at 1.60mm.

In order to see the effects of the motor on driving a gear, the simulation was run using Finite Element Analysis in SolidWorks with a torque applied at the dowel pin holes and holding a tooth face fixed. For the sake of brevity, the directions were chosen to demonstrate the worst case deformations for a given application.

Disclaimer: The author's familiarity with FEA simulation is limited, and they have not yet completed that unit of study at UWA. Therefore, careful consideration of these results should be made before making use of the results in future work.

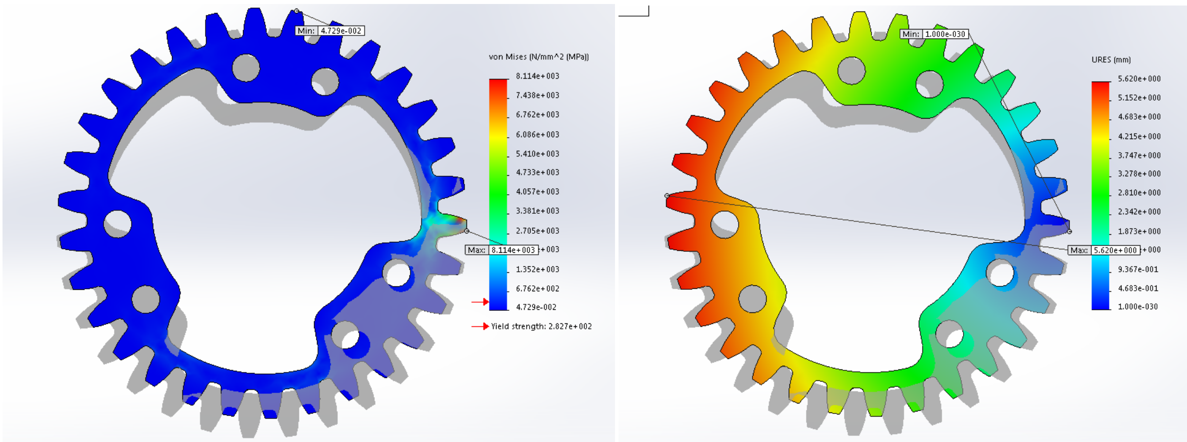

Figure 11 – Torque applied at dowel pins with tooth fixed. The highest displacement is 4.0e+0 mm

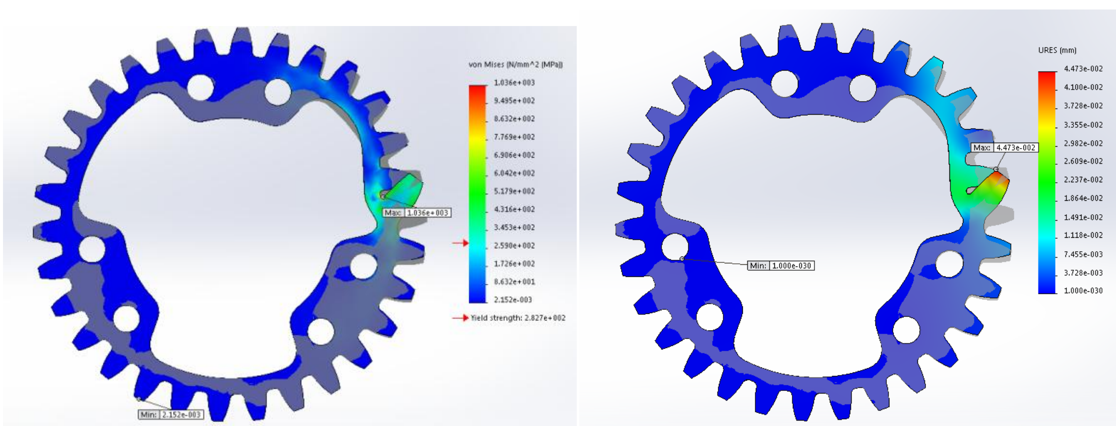

Figure 12 – Torque applied at tooth with dowel pins fixed

4.1.3 Separation force

From (Standards1403, 2011) the tangential force can be calculated:

$$F_t = \frac{torque}{pitch\ diameter/2}$$

$$= \frac{13.87}{\frac{18.9 * 10^{-3}}{2}}$$

$$= 1.47kN$$

The radial separation force of the gear is given by:

$$F_r = F_t * \frac{\tan(radial\ pressure\ angle)}{\cos(axial\ pressure\ angle)}$$

Since the gears are straight cut, the axial pressure angle is 0.

$$F_r = 1.47 * \tan(14.5)$$

$$= 0.38kN$$

4.1.4 Dowel pins in shear

3mm dowel pins are used to locate the gear laminations, as well as distribute the load evenly among a stack of gears. 8mm dowel pins are used to locate planet gears within the bearings on the y-piece. The shear load capacity of a dowel pin (hardened alloy steel) can be determined from the information provided in the Viewmold Technical Data below.

DIMENSIONS | **APPLICATION DATA**

nominal size	A pin diameter		B point diameter		C crown height	R crown radius	calculated single shear strength		recommended hole size	
	max.	min.	max.	min.	max.	min.	kN	pounds	max.	min.
3	3.008	3.003	2.9	2.6	0.8	0.3	7.4	1,670	3.000	2.987
4	4.009	4.004	3.9	3.6	0.9	0.4	13.2	2,965	4.000	3.987
5	5.009	5.004	4.9	4.6	1.0	0.4	20.6	4,635	5.000	4.987
6	6.010	6.004	5.8	5.4	1.1	0.4	29.7	6,650	6.000	5.987
8	8.012	8.006	7.8	7.4	1.3	0.5	52.5	11,850	8.000	7.987
10	10.012	10.006	9.8	9.4	1.4	0.6	82.5	18,550	10.000	9.987
12	12.013	12.007	11.8	11.4	1.6	0.6	119.0	26,700	12.000	11.985
16	16.013	16.007	15.8	15.3	1.8	0.8	211.0	47,450	16.000	15.985
20	20.014	20.008	19.8	19.3	2.0	0.8	330.0	74,000	20.000	19.983
25	25.014	25.008	24.8	24.3	2.3	1.0	515.0	116,000	25.000	24.983

All dimensions in millimeters.

Figure 13 – Technical Data provided by Viewmold

For the 8mm dowel, single shear; 52.5kN

For the 3mm dowel, single shear; 7.4kN

It is observed that the shear capacity of these components is magnitudes greater than the loads experienced in the system. The availability and reliability of dowel pins allows them to be the most convenient solution for this purpose.

4.1.5 Annulus stiffness

The assumption that the face_width = n * thickness_laminate is only valid seeing that the dowel pins are able to transmit the stress effectively to the surrounding laminates. This is a function of the stiffness of the system interfacing the dowel pins.

Of all the components in the transmission, the annulus gear was the largest and therefore most suitable for weight-saving measures. This however causes significant stiffness issues when compared smaller gears where weight-saving is not so beneficial or easy to perform. To investigate this, a number of simulations were performed according to varying load applications.

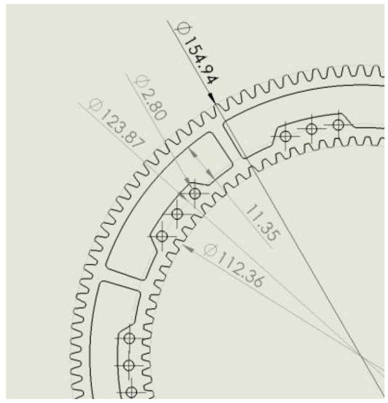

Figure 14 – Major dimensions of the annulus and weight-saving measures for refernece

4.1.5.1 Elongation externally

The elongation of the annulus due to external radial gear force was simulated. Load was applied on the topmost tooth and the fixture was placed at the lowermost dowel hole.

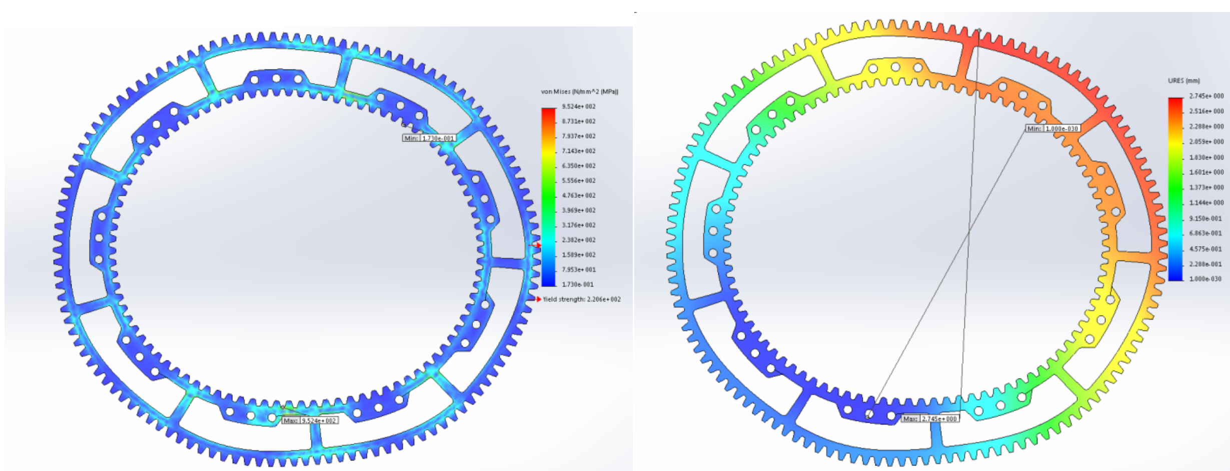

Figure 15 – The annulus under 0.38kN vertical load, the highest deformation experienced is 2.745e+0 mm. The displacement of the point of load application is 1.83e+0 mm.

Next we look at the deformation of the gear segment at the arc over a dowel pin.

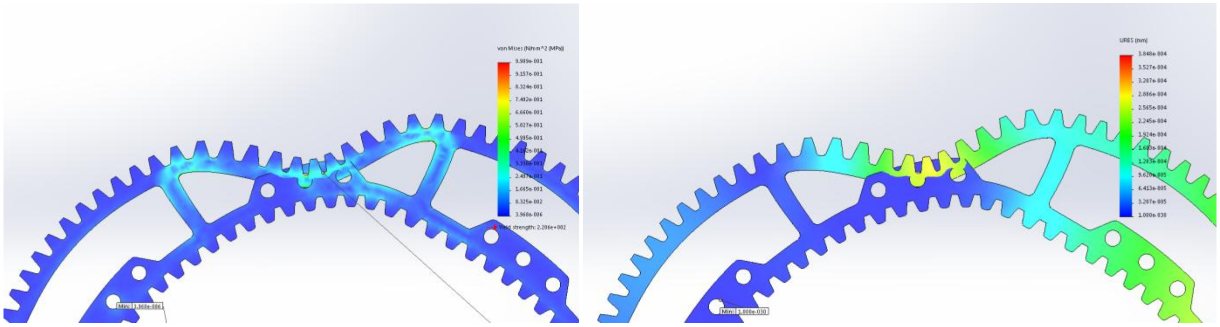

Figure 16 – The deformation of the gear segment under a small load to examine the deformation characteristics. The simulation under 0.38kN would not complete due to a large displacement occurring.

4.1.5.2 Elongation internally

The elongation from internal separation force is also simulated. For simplicity, and to represent a worst case load, only one force is applied as opposed to three (there are three planet gears).

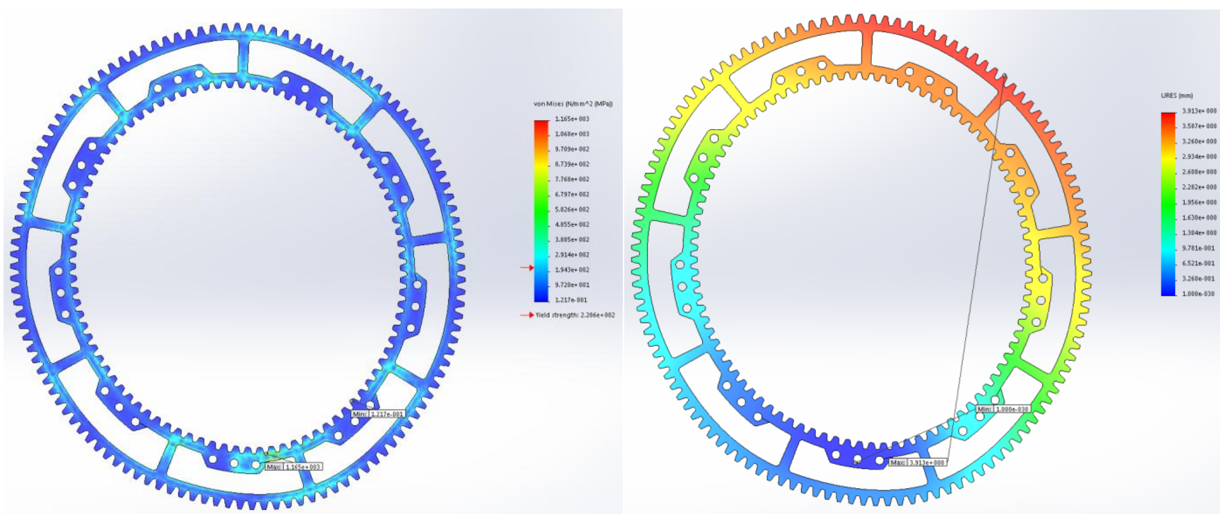

Figure 17 – Elongation under 0.38kN load. The highest elongation is 3.19e+0 mm, and the point of load application is approximately 3.26e+0 mm displacement.

It is clear that a small amount of extra reinforcing of the annulus is called for in order to handle the peak loads of the motors. This is especially important for the arc gear segment as the dowel pins are not able to assist in distributing the load.

4.1.6 Crown Piece stiffness

As similar simulations would be conducted for the crown piece as for the annulus, it is also clear that the crown piece design needs revising. This is recommended as future work.

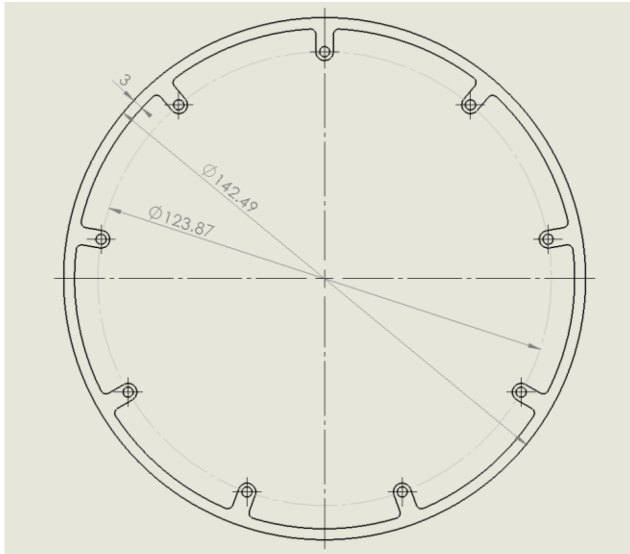

Figure 18 – The crown piece pictured for reference

4.1.7 Y-Piece stiffness

The Y-Piece holds the three planet gears and outputs torque via six 3mm dowel pins. The ability of this design to transmit the torque required can be simulated.

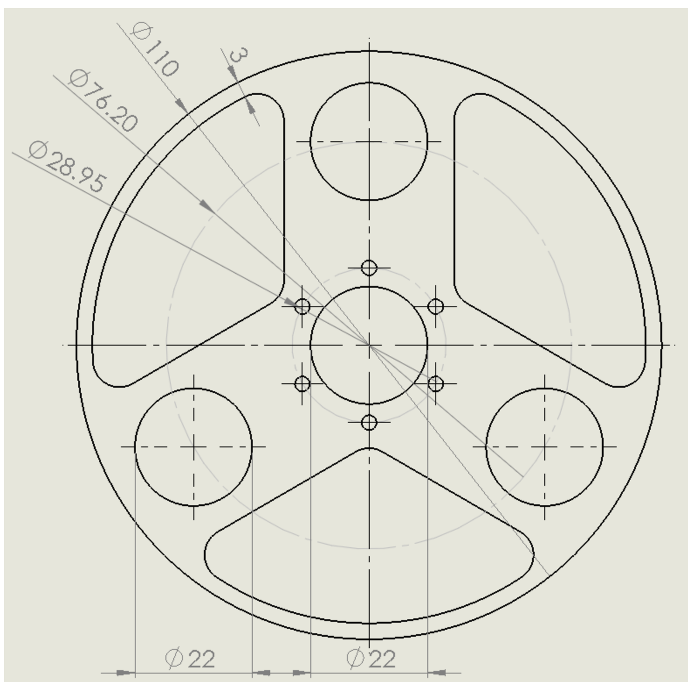

Figure 19 – The Y-Piece

The torque applied is calculated as four times the input torque; 4x41.6 = 166.4Nm. Additionally, the Y-piece is made up of two 3mm steel sheets to ease the complexity of manufacturing as with the gears. Therefore the torque applied by the planets is 166.4/2 = 83.2Nm.

Either the tyre maximum tractive load or braking load of the brakes would be reasonable design criteria for reaction loading. However, it would still be prudent to design the system to withstand a stalling force, as one would expect the brakes to be able to overcome the output torque of the vehicle. With this in mind, the following simulations have been performed by holding the geometry of the output fixed.

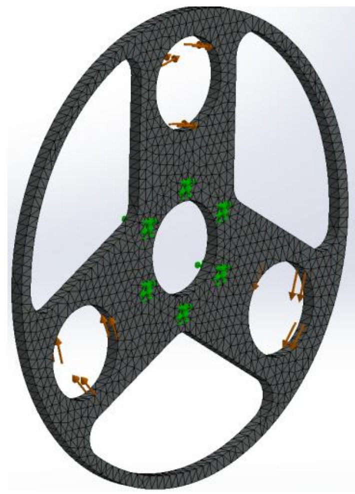

Figure 20 - The loading conditions for the Y-Piece.

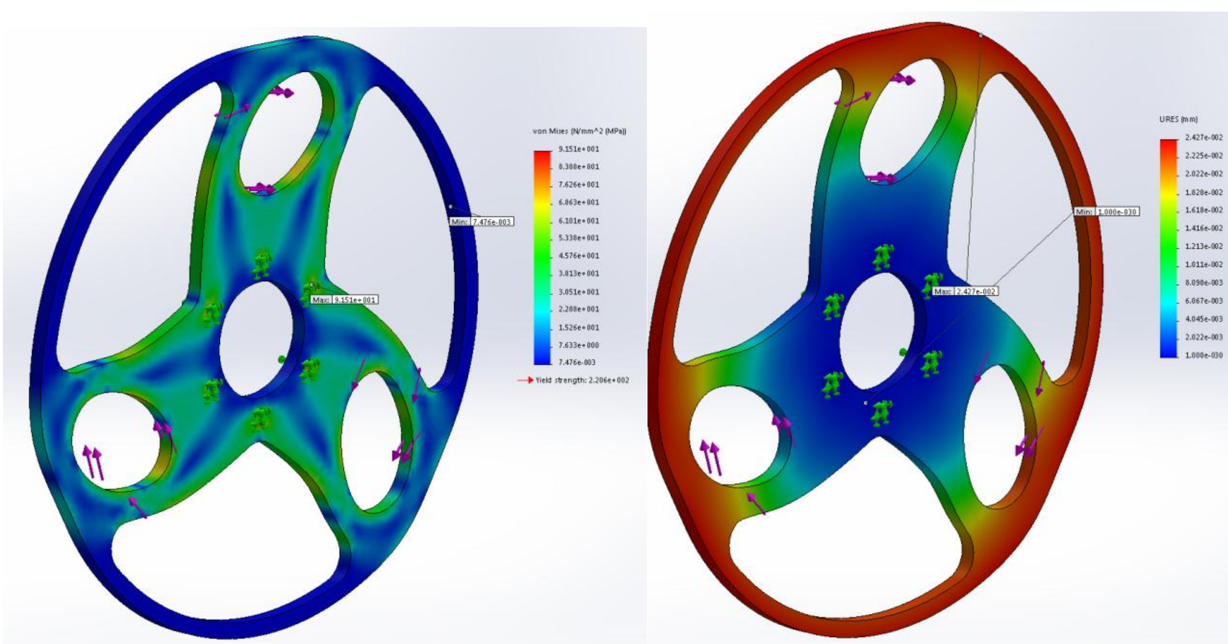

Figure 21 - The Y-Piece under 83.2Nm with the six dowel pins fixed. The highest deformation experienced is 2.43e-2 mm.

After close observation, it is clear that the deformation at the dowel holes is not well represented. An inverted load condition simulation has been included below.

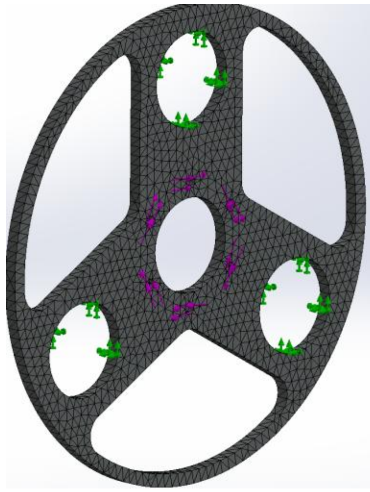

Figure 22 - The inverted loading conditions for the Y-piece.

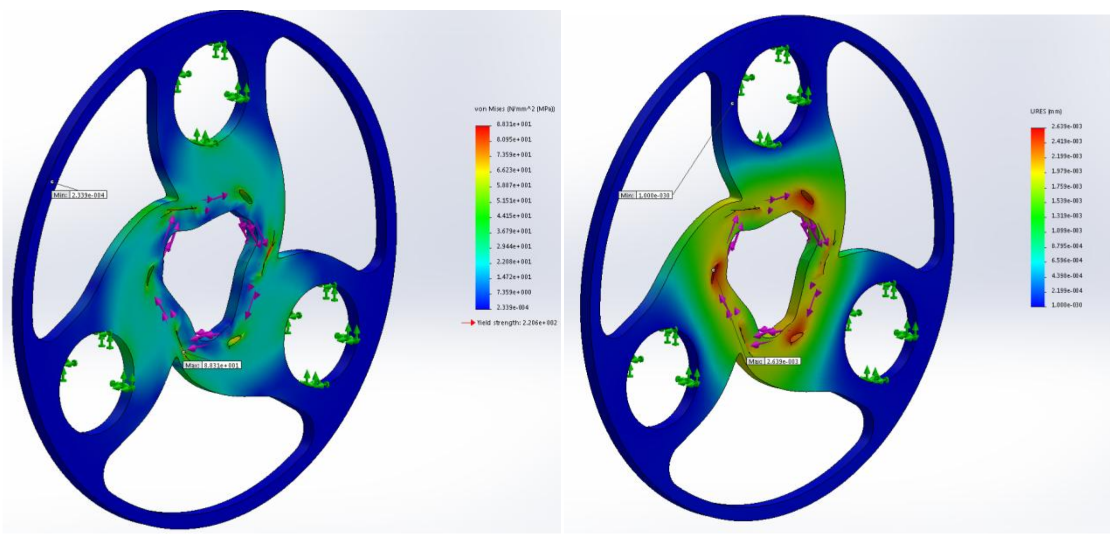

Figure 23 - The inverted results. The highest deformation is 2.64e-3 mm

The Y-Piece also needs to maintain the separation between the planet gears and the drive gear. This implies that the respective bearing holes need to withstand the separation force of the two gears involved.

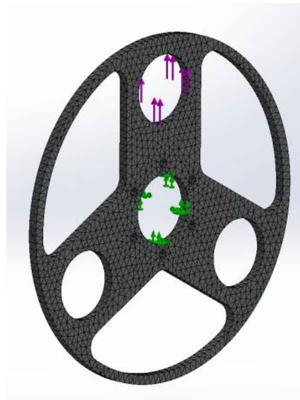

Figure 24 - The loading conditions for separating the centre and topmost bearing holes with 0.38kN

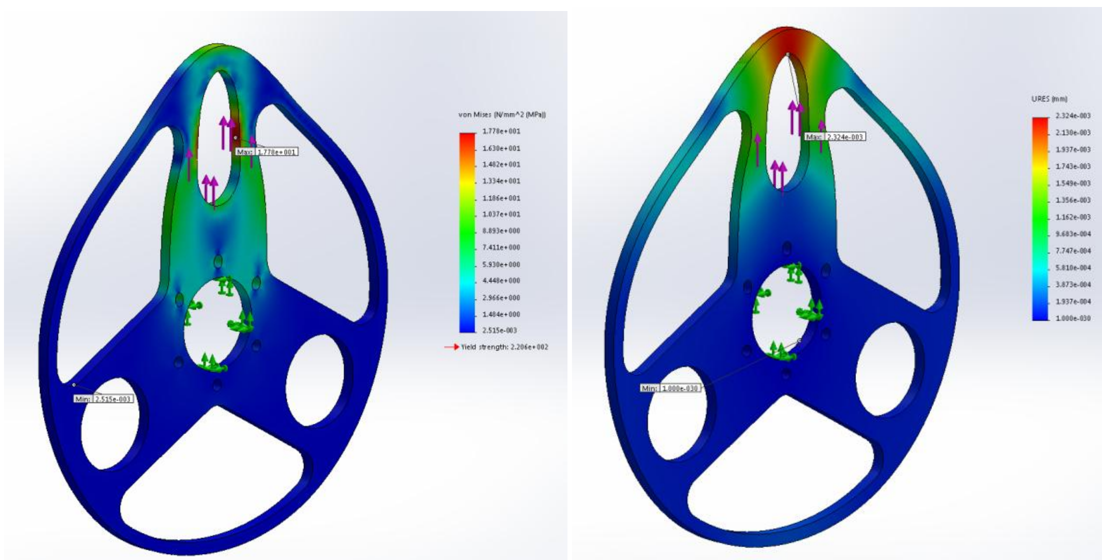

Figure 25 - The results of planetary deformation. The highest deformation is 2.32e-3 mm

The Y-Piece appears well designed to handle the loads it is expected to be subjected to.

5 Test the design for operational suitability and report findings

The testing of this design was planned, however was not completed due to electrical problems. Insight during the assembly and testing were recorded and are included in this report as future work.

A brief summary of the assembly and run-in process is included below

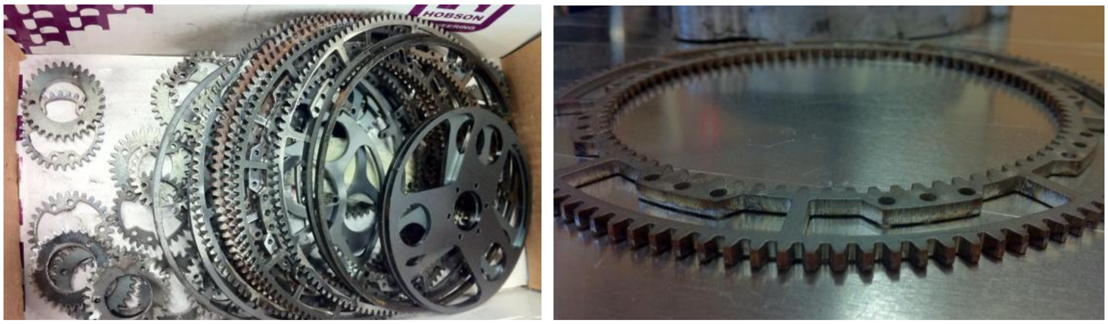

Figure 26 – The laser cut components are received. It is clear that the surface finish and geometry are both very poor. This will do fine for the short operating life expected of the device, however to minimise the probability of fracture initiation due to rough laser kerf, each gear tooth fillet was sandblasted.

Figure 27 – (Left) The case is machined aluminium alloy, generously manufactured through sponsorship by Westurn Engineering in Mandurah, WA.
(Right) The bearings purchased are a standard sized 8x22x7mm bearing (commonly found in skateboards). They are available for ~$2.75 each. The 8mm dowel pin shown was also press fit into the bearing.

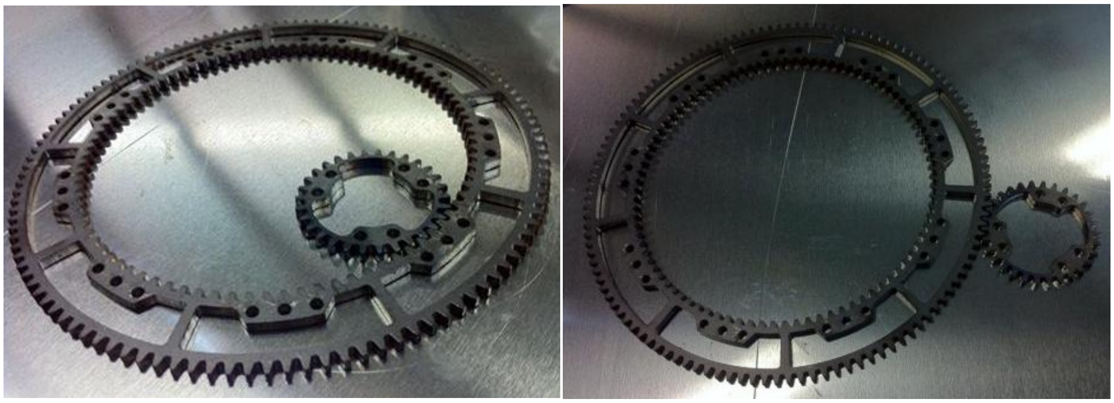

Figure 28 – The fit and meshing of the gears is sufficient for operation. Some flashing was present from the laser cutting, which required hand-finishing. The 3mm dowel holes were laser cut smaller so that they could be drilled to 3mm for an accurate fit.

Figure 29 – (Above and below) The gears were run in after assembly. They mesh smoothly as anticipated. Some small problems with assembly occurred, especially where some laser cut components were bent out of shape due to handling. On observation, some teeth are slightly out of alignment, yet the gears mesh satisfactorily.

6 Propose a system that incorporates the propulsion design into the wheel assembly (Recommendations for future work)

Obviously from the analyses, the transmission needs to be reviewed to handle higher peak loads. As for the remainder of the in-wheel design, it can be shown that the current progress will fit into the wheel without great difficulty.

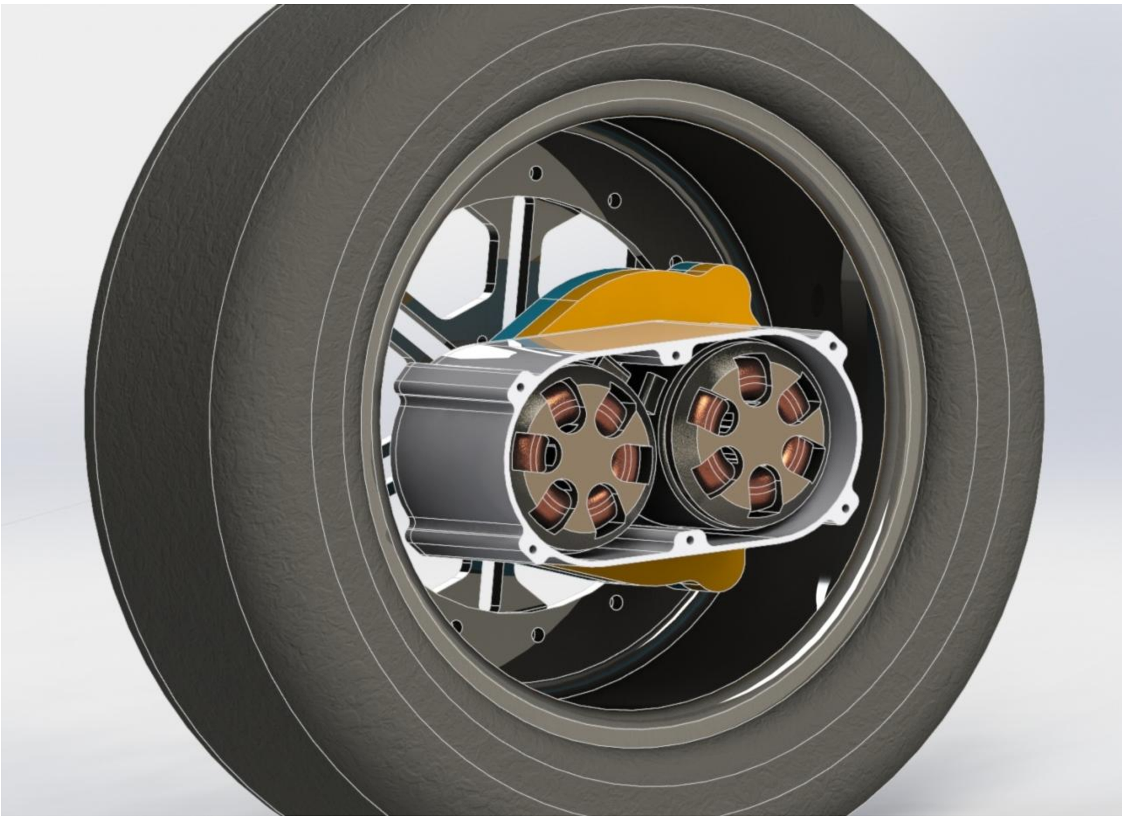

6.1.1 Motor mounting

Motor mounting plates should be considered, and they could be integrated with the motor casing (discussed below).

6.1.2 Motor casing

Excerpt from 2014 Formula SAE Rules:

"EV2.1.2 Motors must be contained within a structural casing where the thickness is at least 3.0 mm (0.120 inch). The casing must use an Aluminum Alloy of at least 6061-T6 grade or better if a casing thickness of 3.0mm is used. If lower grade alloys are used then the material must be thicker to provide an equivalent strength."

As presented in the render above, the case is a 3mm wire EDM structure.

6.2 Propulsion mechanism

Improvements for the Mk IV Prototype of the propulsion mechanism have been observed and are summarised below:

6.2.1 Transmission case

- Case sealing against oil to perhaps Ingress Protection 68
    - O-Ring around case
    - Sealed bearings on motor shaft couplers
- Rotate crown piece bearings to be parallel with a flat datum to reduce the size of pre-machining material required
- Mill lubricant pockets in all sliding surfaces
- Give loose fit for all sliding surfaces such as Y-Piece
- Lubricate with 75W-90 oil
- Backup annulus, crown piece etc. where deflection was found to be a problem

6.2.2 Gear tooth modifications

To reduce overmeshing and run-in time, the small 30-tooth gears should be clipped by perhaps 0.2mm. This also increases the void that captures lubricant between gears.

The teeth that are clipped should have radii specified to reduce contact stress on initial gear tooth contact.

6.3 In-wheel assembly

A reliable method must be found of securing the wheel to the in-wheel assembly. It must also feature a positive-locking mechanism (as per the rules) such as nyloc nuts, cotter pins, or safety locking wire.

As for the upright (spindle retaining suspension component), the in-wheel assembly is so volumetrically large that it would be sensible to mount suspension hardpoints directly to the transmission cases. Even if additional structure is required, the saving of an entire upright component would certainly make for more efficient use of material within the assembly.

6.3.1 Spindle design, bearings and wheel centre

Due to the size of the wheel centre and the requirements for it to be as light as possible, wire EDM is favoured as the machining process. This however means that the number of penetrations should be minimised as part of the design. The wheel centre featured in the render above has been designed to only feature two penetrations to complete all 12 spoke elements.

The initial designs for the spindle involved turning on a lathe. The major problems encountered were large quantities of material needing removal, and complex geometries needing to be machined. Any wheel locking mechanism associated with this was also relatively complex and expensive to machine. It was then proposed that to avoid this, a 12.9 grade high tensile M36x900mm bolt with an M36 nyloc nut would be an economic way to ensure the axial and bending capacity of the spindle, and a reliable and cost-effective wheel locking mechanism. The bolts are available for ~$63 each, which is less than even one hour of workshop time.

6.3.2 Brake caliper and rotor

Another important consideration that follows from (Hooper, 2011) is that the brake rotor should be mounted on the wheel-side of the transmission. This is to ensure that braking effectiveness is maintained even in the event of a transmission or shaft failure.

7 Bibliography

Anon, (2014). 1st ed. [ebook] Available at: http://viewmold.com/Products/Unbrako-Screw/Metric%20Dowel%20Pins.pdf [Accessed 31 Oct. 2014].

Mraz, S. (2013). *Hub Motors for All-Electric Vehicles Still Have Some Technological Challenges to Overcome | Automotive content from Machine Design*. [online] Machinedesign.com. Available at: http://machinedesign.com/automotive/hub-motors-all-electric-vehicles-still-have-some-technological-challenges-overcome

Rushgears.com, (2014). *RushGears.com -- Nobody Makes Custom Gears Faster*. [online] Available at: http://rushgears.com (BR Enclosures) http://www.brenclosures.com.au/pdfs/ip-rating-chart.pdf

Fsae.com, (2014). *FSAE.com*. [online] Available at: http://www.fsae.com/results.shtml [Accessed 31 Oct. 2014]. (Protean) http://green.autoblog.com/2013/04/17/protean-electric-production-ready-in-wheel-electric-drive/

Patentscope.wipo.int, (2014). *IB2011050477 STATOR WITH RADIALLY MOUNTED TEETH*. [online] Available at: http://patentscope.wipo.int/search/en/detail.jsf;jsessionid=5D1D338FF0DA54F68A9312E76D5C17CA.wapp1nA?docId=WO2011095945&recNum=1&tab=Drawings&maxRec=&office=&prevFilter=&sortOption=&queryString

GERLING, D., DAJAKU, G. and LANGE, B. (2013). *ELECTRIC TRACTION FOR AUTOMOBILES - COMPARISON OF DIFFERENT WHEEL-HUB DRIVES*. [online] Available at: http://www.proteanelectric.com/en/wp-content/uploads/2013/07/protean-Services2.pdf

Standards1403, A. (2011, 05 02). AS1403-2004. Rotating steel shafts. Standards Australia.

Dokumente.unibw.de, (2014). Traction Drives for Passenger Cars [online] Available at: https://dokumente.unibw.de/pub/bscw.cgi/2221268 [Accessed 31 Oct. 2014].

Hooper, I. (2011). *Development of In-Wheel Motor Systems for Formula SAE Electric Vehicles*. Masters of Engineering. University of Western Australia.

Larminie, J. and Lowry, J. (2003). *Electric vehicle technology explained*. West Sussex, England: J. Wiley.

Fullermetric.com, (2014). *Mechanical Properties | Fuller Metric Parts Ltd.*. [online] Available at: http://www.fullermetric.com/technical/information/tech_mechanical_properties.aspx

8 Appendices

Material properties

Materials in the default library can not be edited. You must first copy the material to a custom library to edit it.

Model Type: Linear Elastic Isotropic

Units: SI - N/m^2 (Pa)

Category: Steel

Name: Plain Carbon Steel

Default failure criterion: Max von Mises Stress

Description:

Source:

Sustainability: Defined

Property	Value	Units
Elastic Modulus	2.1e+011	N/m^2
Poisson's Ratio	0.28	N/A
Shear Modulus	7.9e+010	N/m^2
Mass Density	7800	kg/m^3
Tensile Strength	399826000	N/m^2
Compressive Strength		N/m^2
Yield Strength	220594000	N/m^2
Thermal Expansion Coefficient	1.3e-005	/K
Thermal Conductivity	43	W/(m·K)
Specific Heat	440	J/(kg·K)
Material Damping Ratio		N/A

Material properties

Materials in the default library can not be edited. You must first copy the material to a custom library to edit it.

Model Type: Linear Elastic Isotropic

Units: SI - N/m^2 (Pa)

Category: Aluminium Alloys

Name: 6061-T6 (SS)

Default failure criterion: Max von Mises Stress

Description:

Source:

Sustainability: Defined

Property	Value	Units
Elastic Modulus	6.900000067e+010	N/m^2
Poisson's Ratio	0.33	N/A
Shear Modulus	2.600000013e+010	N/m^2
Mass Density	2700	kg/m^3
Tensile Strength	310000002.1	N/m^2
Compressive Strength		N/m^2
Yield Strength	275000000.9	N/m^2
Thermal Expansion Coefficient	2.4e-005	/K
Thermal Conductivity	166.9	W/(m·K)
Specific Heat	896	J/(kg·K)
Material Damping Ratio		N/A

(Solidworks Simulation 2014)

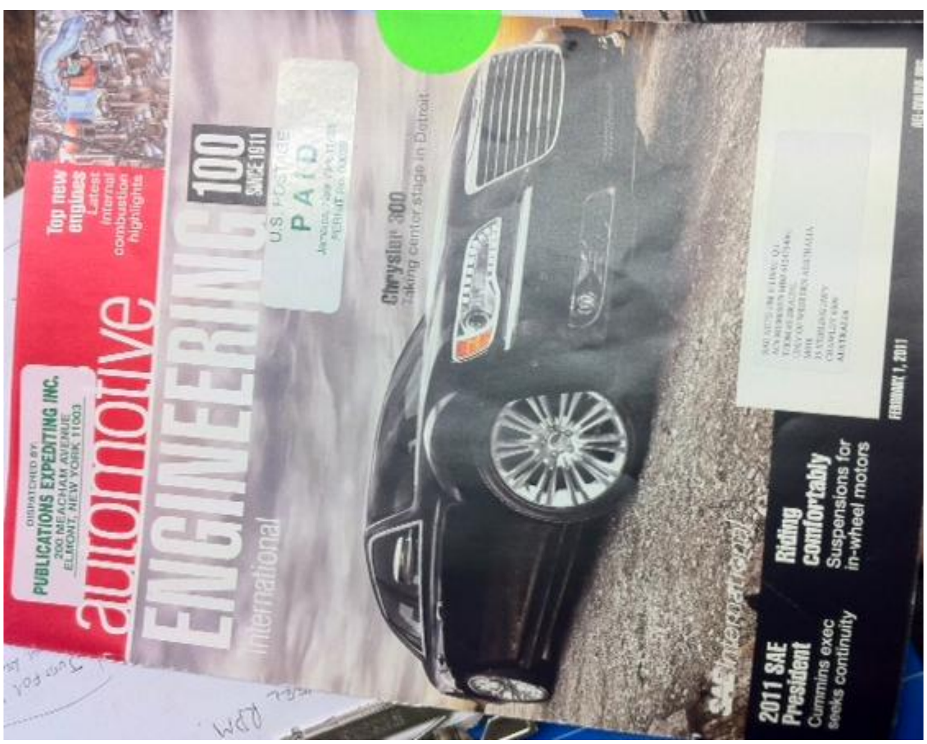

Rules Excerpts from Formula SAE 2014:

EV2.3.4 At least two separate sensors have to be used as torque encoder. Separate is defined as not sharing supply or signal lines.

EV2.3.5 If an implausibility occurs between the values of these two sensors the power to the motor(s) must be immediately shut down completely. It is not necessary to completely deactivate the tractive system, the motor controller(s) shutting down the power to the motor(s) is sufficient.

EV2.3.6 Implausibility is defined as a deviation of more than 10% pedal travel between the sensors.

EV2.3.9 The torque encoder signals must be sent directly to a controller using an analogue signal or via a digital data transmission bus such as CAN or FlexRay. Any failure of the sensors or sensor wiring must be detectable by the controller and must be treated like an implausibility, see EV2.3.5. This implausibility must either be directly detected by the motor controller or transmitted to the motor controller such that power from the motor controller to the motor(s) is immediately and completely shut down.

EV2.3.10 When an analogue signal is used, eg. from a 5V sensor, the torque encoder sensors will be considered to have failed when they achieve an open circuit or short circuit condition which generates a signal outside of the normal operating range, for example <0.5V or >4.5V. The circuitry used to evaluate the sensor will use pull down or pull up resistors to ensure that open circuit signals result in a failure being detected.

EV2.3.11 When any kind of digital data transmission is used to transmit the torque encoder signal, the FMEA study must contain a detailed description of all the potential failure modes that can occur, the strategy that is used to detect these failures and the tests that have been conducted to prove that the detection strategy works. The failures to be considered must include but are not limited to the failure of the sensor, sensor signals being out of range, corruption of the message and loss of messages and the associated time outs. In all cases a sensor failure in a two sensor setup must result in power to the motor(s) being immediately shutdown as per the implausibility requirements of EV2.3.5.

EV2.3.12 Any algorithm or electronic control unit that can manipulate the torque encoder signal, for example for vehicle dynamic functions such as traction control, may only lower the total driver requested torque and must never increase it. Thus the drive torque which is requested by the driver may never be exceeded.

EV2.5 Torque Encoder / Brake Pedal Plausibility Check

The power to the motors must be immediately shut down completely, if the mechanical brakes are actuated and the torque encoder signals more than 25% pedal travel at the same time. This must be demonstrated when the motor controllers are under load.

EV2.5.1 The motor power shut down must remain active until the torque encoder signals less than 5% pedal travel, no matter whether the brakes are still actuated or not.

EV5.6 Brake System Plausibility Device

A standalone non-programmable circuit must be used on the car such that when braking hard (without locking the wheels) and when a positive current is delivered from the motor controller (a current to propel the vehicle forward), the AIRs will be opened. The current limit for triggering the circuit must be set at a level where 5kW of electrical power in the DC circuit is delivered to the motors at the nominal battery voltage. The action of opening the AIRs must occur if the implausibility is persistent for more than 0.5sec. This device must be provided in addition to the plausibility checks which are carried out by the controller which interprets the drivers torque request and delivers torque to the wheels. The Brake Plausibility Device may only be reset by power cycling the GLVMS.

The team must devise a test to prove this required function during Electrical Tech Inspection. However it is suggested that it should be possible to achieve this by sending an appropriate signal to the non-programmable circuit that represents the current to achieve 5kW whilst pressing the brake pedal to a position or with a force that represents hard braking.

(9) VAN DER SPUIJ, R. S.: 'Underground Locomotive Practice', New Consolidated Gold Fields Ltd. Handbook, October, 1951.

(10) POGGI, L.: 'Il Complesso Motori "in Pariglia" e la sua Applicazione ai Locomotori di Manovra', Istituto di Fisica Tecnica della Facoltá di Ingegneria, Pisa, 52 Riunione Annuale dell Associazione Elettrotecnica Italiana, Firenze, September, 1951.

(11) PRIGMORE, B. J.: 'The Rating and Service Capacity of Traction Motors', *Proceedings I.E.E.*, Monograph No. 65, June, 1953 (**100**, Part IV, p. 91).

(12) SAY, M. G., and FRAMPTON, H. G.: 'The Compound Characteristic in Regenerative Braking with Direct Current Traction', *Journal I.E.E.*, 1923, **61**, p. 863.

(13) SMITH, R. M.: 'Locomotive Wheel Slip and Wheel Lock Protection', *Transactions of the American I.E.E.*, 1950, **69**, Part II, p. 1154.

(14) SYKES, J. H. M.: 'Progress towards 50-cycle Railway Electrification', *BEAMA Journal*, December, 1953.

(15) SYMES, H. E. J.: 'A Differential Drive for Electric Locomotives', *Transactions of the South African Institute of Electrical Engineers*, 1955, **46**, p. 296.

(8) APPENDICES

(8.1) Speeds and Torques in the Differential Gear

A full analysis of the behaviour and characteristics of the epicyclic differential gear with regard to speeds and torques of the three elements for all the epicyclic inversions is given in Reference 7. However, Fig. 13 indicates briefly the more important aspects of the transmission which affect the two machines and the output.

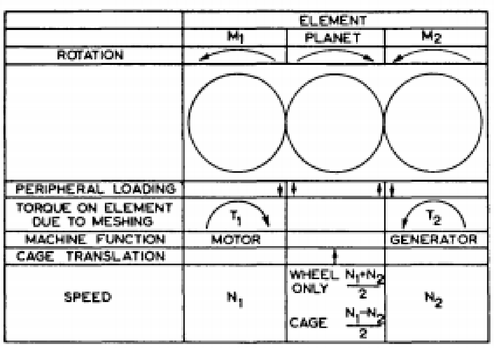

Fig. 13.—Conditions through epicyclic gear.

For clarity, the gears coupled to the machines M_1 and M_2 and one of the multiple planetary wheels are shown as co-planar. To ensure rotation of the planetary unit only without translation of its axis when the machine speeds are equal, i.e. for idling, the directions of rotation of M_1 and M_2 must be as shown. If the bodily movement of the planetary unit is restrained by the mechanical load on the drive while the speed of M_1 is increased by shunt field adjustment, it follows that the speed of M_2 must also be raised whilst its field is constant. The function of the latter machine is thus changed by the load from motoring to generating.

This feature is also apparent from an examination of the torque distribution. Reference to Fig. 13 indicates that, whereas the rotation and torque of the motor element M_1 are in opposite directions, those of M_2 are in the same direction, making M_2 a generator.

In any form of epicyclic differential unit which is mechanically symmetrical with respect to the two machines it is apparent that the two peripheral or tangential loads on the planetary wheel must be equal under steady conditions. It therefore follows that the torques on M_1 and M_2 are always of the same magnitude, or $T_1 = T_2$ numerically. Hence, the power associated with each machine is directly proportional to its speed.

It may be seen from the complete differential assembly (Fig. 1) that the machines rotate in opposite directions with respect to the differential while they function as motor and generator under load. The torques applied by both machines to the cage are therefore in the same direction or additive. This fact is also indicated in Fig. 13, where it is seen that the two peripheral loads on a plantetary unit at the ends of its meshing diameter are in the same direction. The driving reaction at the axis of the planetary wheel is thus the sum of these two loads.

The following relationship is then obtained:

$$T = T_1 + T_2 = 2T_1 = 2T_2$$

Since the torques are equal it follows that the power and current of each machine are proportional to its speed, i.e. $P_1/P_2 = N_1/N_2 = I_1/I_2$.

The motor-generator condition is present whenever the drive is loaded, irrespective of whether the locomotive is stationary or moving, or whether braking or tractive effort is developed at the road wheels.

For the speed relationships it is seen from Fig. 13 that the output speed of the cage is $(N_1 - N_2)/2$.

(8.2) Some Properties of the Circle (Section 3.3)

The general equation of a circle is

$$x^2 + y^2 + 2gx + 2fy + c = 0$$

Compared with the expression obtained in Section 3.3, this gives $g = V^2S_1/2t$ and $f = - V^2S_2/2t$. The radius is $\sqrt{(g^2 + f^2 - c)}$ which becomes $V^2\sqrt{(S_1^2 + S_2^2)}/2t$, since c is zero. In the absence of c the curve is constrained to pass through the origin.